Available online at www.sciencedirect.com

ScienceDirect

Proceedings of the Combustion Institute 000 (2022) 1–11

Proceedings of the Combustion Institute

www.elsevier.com/locate/proci

Critical conditions at liftoff limit of a laminar n-butane-air jet diffusion flame

Fumiaki Takahashi [a,*], Logan Smith [a], Daniel T. Souza [a], Viswanath R. Katta [b]

[a] *Case Western Reserve University, Mechanical and Aerospace Engineering, 10900 Euclid Avenue, Cleveland, OH 44106, USA*

[b] *Innovative Scientific Solutions, Inc., Dayton, OH 45440, USA*

Received 6 January 2022; accepted 2 July 2022
Available online xxx

Abstract

The stability mechanism of laminar coflow jet diffusion flames in normal gravity has been studied computationally and experimentally. N-butane, the heaviest alkane in a gaseous state at ambient temperature and pressure, is used as the fuel since the reaction mechanism is similar to that of higher (liquid) hydrocarbons. The critical mean n-butane jet and coflowing air velocities at flame stability limits are measured using a small fuel tube burner (0.8 mm inner diameter). The time-dependent, axisymmetric numerical code with a detailed reaction mechanism (58 species and 540 reactions), molecular diffusive transport, and a radiation model, reveals a flame structure. A fuel-lean peak reactivity spot (i.e., *reaction kernel*), possessing the hybrid nature of diffusion-premixed flame structure at a constant temperature of ≈1560 K, is formed at the flame base and controls the flame stability. In a near-quiescent environment, the flame base resides below the fuel tube exit plane and thereby premixing is limited. As the coflowing air velocity is increased incrementally under a fixed fuel jet velocity, the flame base moves slightly above (≈1 mm) the burner exit and vigorous premixed combustion becomes prevailing. The local heat-release rate at the reaction kernel nearly doubles due to the increased convective oxygen flux (i.e., a blowing effect). The local Damköhler number, newly defined as a ratio of the square root of the local heat-release rate and the local velocity, decreases gradually first and drops abruptly at a critical threshold value and the flame base lifts off from the burner rim. The calculated coflow air velocity at liftoff is ≈0.38 m/s at the fuel jet velocity of 2 m/s, which is consistent with an extrapolated measured value of 0.41 m/s. This work has determined the critical Damköhler number at the stability limit quantitatively, for the first time, for laminar jet diffusion flames.

Keywords: Laminar diffusion flame structure; Stability limit; Numerical simulation; Reaction kernel; Damköhler number

* Corresponding author.
E-mail addresses: fxt13@case.edu, fumiaki.takahashi-1@nasa.gov (F. Takahashi).

https://doi.org/10.1016/j.proci.2022.07.037
1540-7489 © 2022 Published by Elsevier Inc. on behalf of The Combustion Institute.

1. Introduction

The stability and structure of coflow diffusion flames have long been frequent subjects of research since the early years of modern combustion science [1–3]. Flame holding and blowoff phenomena are of essential importance in relation to efficient and stable operation of combustion systems as well as fire safety issues. Stability characteristics of coflow diffusion fames have been investigated extensively for various experimental systems (burner design, types of fuel, inert gas, and inhibitor) and boundary conditions (velocity, temperature, oxygen, and gravity) [4–32].

Although there are numerous papers on the lifted diffusion flames, only few are concerned about the stabilization and destabilization of burner-rim attached flames leading to liftoff (then blowout) or blowoff directly. The stability mechanism of diffusion flames is less understood mainly because of lack of characteristic parameters like laminar flame speed of premixed flames. A conventional view of attached diffusion flame postulates [3], "there must be a sort of flame velocity in this premixed zone at the base which causes the combustion processes to propagate downwards along the flame front against the gas stream, thus preventing the flame from lifting." A lifted flame with its base sufficiently far from the burner (typically in several cm order) is known to form, under certain conditions, a triple-flame (or tribrachial) structure [9,11,12], i.e., a stoichiometric diffusion flame with a triple point at its base with fuel-lean and fuel-rich premixed flame branches. The triple flame propagates against the fuel-air mixture flow to make it stationary. Fuel chemistry can significantly affect the stabilization process and low-temperature chemistry could lead to multi-brachial flame structures [28].

As a result of significant advances in reaction mechanisms and computational capabilities in the past few decades, it has become feasible to perform, albeit time consuming, unsteady computation with full chemistry in simple configurations (burner geometry, flow, and fuel) with confidence. In a series of previous papers [13-18,21-23,26,27,30,32], for more than two decades, we reported results of computation of the structure of the flame-stabilizing base region of diffusion flames of C_1 to C_3 hydrocarbons. It was found that a peak reactivity spot, i.e., reaction kernel, played a critical role in flame holding, detachment, oscillation, and blowoff of the trailing diffusion flame. In these studies, methane, ethane, ethylene, acetylene, and propane were used as the fuels. In the attached flames, the space between the flame base and the burner rim (typically in a 1 mm order) as well as the fuel-air mixing layer's lateral thickness are not sufficient to form the triple flame structure [14-16,18]. In the flame propagation study for C_2 hydrocarbons [17], the triple flame structure was formed for the fuels with wide rich flammability limit (acetylene and ethylene), but the fuel-rich branch was missing for the alkanes.

The reaction kernel is at the fuel-lean condition because of the significant oxygen leakage (2–5%) through the reaction zone and thus the convective oxygen flux (i.e., concentration × velocity) boosts up the heat-release (or oxygen-consumption) rate. Therefore, the local equivalence ratio at the reaction kernel depends on the oxygen concentration, velocity, and thus the location of the reaction kernel itself. If the flame base shifts to an upper (fuel leaner and faster) stable location, the local equivalence ratio decreases. The reaction kernel hypothesis for the stability limit of laminar jet diffusion flames proposed in our previous studies [14,15] was valid qualitatively. The current study attempts to evaluate the critical Damkhöler number (Da) at the reaction kernel quantitatively.

In this paper, n-butane (C_4 hydrocarbon) is used as the fuel, for the first time, because it is the heaviest alkane gas at ambient temperature and pressure, the reaction mechanism is similar to that of higher (liquid) hydrocarbons and readily available, and it is used for a wide range of products (e.g., lighters, stoves, aerosols, heating, and refrigerant). The density of butane is 3.6 × larger than methane, resulting in a lower kinematic viscosity, higher jet Reynolds number (Re_j), and thus affecting the equivalence ratio at the reaction kernel as well as the fluid mechanic aspect of the flame stabilization.

The present ground-based research extends the first phase of the NASA Structure and Liftoff In Combustion Experiment (SLICE) project [29] conducted in microgravity aboard the International Space Station. It also relates to the previous fire-suppression studies [22,23,26,27,30,32] by chemically passive and active fire-extinguishing agents. The objectives of this study are (1) to reveal the structure of the rim-attached laminar coflow diffusion flame in a near-quiescent environment to understand the flame holding mechanism, (2) to investigate the effects of coflow air velocity on physical and chemical structure, and (3) to determine the flame detachment (liftoff or blowoff) limit conditions controlling the stability mechanism, by using n-butane as the fuel.

2. Experimental procedures

The burner consists of a circular fuel tube (0.76 mm i.d., 0.91 mm o.d.) positioned coaxially inside a glass chimney (9.5 cm inner diameter, 22.5 cm height). Although larger fuel tubes (1.59 mm and 2.14 mm i.d.) have also been used, this paper reports the results of the smallest size only, in which the pipe flow is laminar at liftoff. The gas flow rates are measured by mass flow meters (Hastings HFM-200 [fuel] and HFM-201 or Sierra 930H [air]), which are calibrated so that their uncertainty is 2% of indicated flow. The fuel gas used

Please cite this article as: F. Takahashi, L. Smith, D.T. Souza et al., Critical conditions at liftoff limit of a laminar N-butane-air jet diffusion flame, Proceedings of the Combustion Institute, https://doi.org/10.1016/j.proci.2022.07.037

is n-butane (Airgas CP, 99%), and the air is house compressed air supplied by an oil-free compressor (filtered and dried). For a fixed mean air velocity (U_a), the mean fuel jet velocity (U_j) is increased (in increments of $< 1\%$ near the limit) until the flame liftoff and blowout occurs. The test was repeated 3 times and the average is reported.

3. Computational method

The numerical simulation of coflow diffusion flames stabilized on the fuel tube burner is performed using a time-dependent, axisymmetric numerical code (UNICORN) [33,34]. The code solves the axial and radial (z and r) full Navier-Stokes momentum equations, continuity equation, and enthalpy- and species-conservation equations on a staggered-grid system. The buoyancy effect is included in the momentum equation. A clustered mesh system is employed to trace the gradients in flow variables near the flame surface. The thermophysical properties such as enthalpy, viscosity, thermal conductivity, and binary molecular diffusion of all the species are calculated from the polynomial curve fits developed for the temperature range 300-5000 K. Mixture viscosity and thermal conductivity are then estimated using the Wilke and Kee expressions [35], respectively. Molecular diffusion is assumed to be of the binary-diffusion type, and the diffusion velocity of a species is calculated using Fick's law and the effective-diffusion coefficient of that species in the mixture. A simple radiation model [36] based on the optically thin media assumption is incorporated into the energy equation. Radiation from CH_4, CO, CO_2, and H_2O was considered in this study. The Plank-mean absorption coefficients are obtained from the literature [35]). The finite-difference forms of the momentum equations are obtained using an implicit QUICKEST scheme [33], and those of the species and energy equations are obtained using a hybrid scheme of upwind and central differencing. A reaction mechanism for the simulation of n-butane flames is the San Diego mechanism 2016 release for C_1-C_3 hydrocarbons [37] extended to C_4 [38] (58 species and 540 one-way elementary reactions) and integrated into the UNICORN code.

The computational domain of 50 × 20 mm in the axial (z) × radial (r) directions is bounded by the axis of symmetry, a chimney wall, and the inflow and outflow boundaries. The domain is represented by a mesh of 261 × 81 with clustered grid lines near the axisymmetric jet exit and a minimum spacing of 0.02 mm. The burner tube inner diameter, the lip thickness, and the chimney inner diameter are $d = 0.8$ mm, 0.1 mm, and 40 mm, respectively. The fuel tube exit plane is placed 4 mm downstream from the inflow boundary in the open computational domain. The fuel tube wall temperature is set at 294 K for the inlet portion (2-mm length) and 600 K for the exit portion (2-mm length). Fully developed pipe flow in the fuel tube and boundary layer velocity profiles outside the burner tube are used. The boundary conditions are treated in the same way as reported in earlier papers [14–18].

First, a baseline n-butane jet flame (low fuel and air velocities) was obtained through performing detailed-chemistry calculations on the initial solution generated with the global-chemistry model. Then the required flame solution for the specified fuel and/or air velocities is obtained through gradually increasing the respective velocity component. Flame lift-off conditions for a fixed fuel jet velocity (U_j) of 2 m/s are obtained through increasing the air velocity gradually (in increments of $< 1\%$ near detachment). At each increment, the previous solution is used for the initial data consecutively.

4. Results and discussion

4.1. Stability limit measurement

The laminar diffusion flame base, initially anchored at the burner rim, controls the processes of flame attachment, detachment (liftoff or direct blowoff), and eventually lifted-flame blowout. Fig. 1 shows the measured stability limits of n-butane-air coflow jet diffusion flames. This study focuses on the attachment and detachment of the laminar flame, although the turbulent lifted-flame blowout limits are also shown for completeness. The critical U_j (and converted Re_j) at the liftoff limit are determined as the blue flame base moves away from the burner rim approximately 2 mm. The laminar flame base moves farther away from the burner to form a turbulent lifted flame like the methane flames reported previously [15]. Further increases in the fuel jet velocity results in the lifted-flame blowout limits. The critical U_j's, both at lift and blowout, decrease as U_a is increased due to the destabilizing effect of the coflowing air.

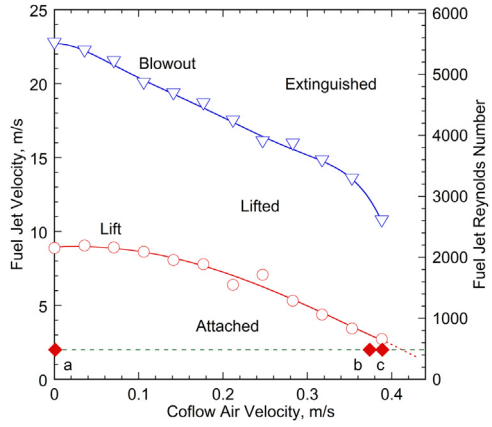

Fig. 1. Measured liftoff and blowout limits of n-butane diffusion flames. $d = 0.76$ mm.

Please cite this article as: F. Takahashi, L. Smith, D.T. Souza et al., Critical conditions at liftoff limit of a laminar N-butane-air jet diffusion flame, Proceedings of the Combustion Institute, https://doi.org/10.1016/j.proci.2022.07.037

4.2. Flame structure

The numerical simulations have been performed at incrementally increased U_a's (a total of 115 conditions) under a constant U_j (2 m/s, which converts to $Re_j = 485$) along a dashed line in Fig. 1. Each computation takes typically 2-4 h, except much longer initial runs. Fig. 2 shows selected cases of the calculated flame structure at three different air velocities ($U_a = 0.01$, 0.374 and 0.389 m/s). The velocity conditions for Fig. 2a-c are shown as "a" "b", and "c" in Fig. 1, respectively. The variables include the velocity vectors (v), isotherms (T), and heat-release rate ($\dot{q}$). In Fig. 2a, the flame base is anchored at the burner rim in a low-velocity air environment. The fuel jet expands downstream as the jet momentum transfers outwardly and entrains the surrounding fluid. As a result, the flame zone depicted as the high heat-release rate zone (rainbow color coded) inclines outwardly like a candle. The coflowing air flow approaches the high-temperature zone and accelerates due to thermal expansion. The heat-release rate contours show a peak reactivity spot (i.e., the *reaction kernel* [15,16,18]) at the flame base below the fuel jet exit plane. The height and the radius at the reaction kernel (the peak $\dot{q}$ point) are $z_k = -0.15$ mm and $r_k = 1.07$ mm, respectively, where subscript k is at the reaction kernel. The values of the variables at the reaction kernel are $|v_k| = 0.309$ m/s, $T_k = 1512$ K, and $\dot{q}_k = 178.8$ W/cm^3, where $|v|$ is the magnitude of the velocity vector v.

For the near-limit flame (Fig. 2b), the flame base is pushed upward by the incoming entrainment flow and the space below the flame base widens, thus promoting the fuel-air mixing. The heat-release rate more than doubled compared to the initial flame (Fig. 2a). The values of the variables at the reaction kernel are $z_k = 0.92$ mm, $r_k = 1.15$ mm, $|v_k| = 0.542$ m/s, $T_k = 1543$ K, and $\dot{q}_k = 430.8$ W/cm^3.

The lifted flame base (Fig. 2c) not only drifts downstream but also moves outwardly. The reaction kernel broadens as the fuel-air mixing layer below the flame base thickens. However, the triple (or tribrachial) flame structure is not formed since the fuel rich branch is not formed similarly to the C_1 through C_3 alkanes as reported previously [17]. The heat-release rate maintains about the same as the near-limit flame (Fig. 2b). The values of the variables at the reaction kernel are $z_k = 4.94$ mm, $r_k = 1.46$ mm, $|v_k| = 0.610$ m/s, $T_k = 1482$ K, and $\dot{q}_k = 404.3$ W/cm^3.

Fig. 3 shows the calculated radial variations of (a) the temperature and the heat-release rate and (b) the axial (U) and radial (V) velocity components across the reaction kernel for three different U_a's, corresponding to Fig. 2a-c, respectively. In Fig. 3a, for all cases, the peak temperatures are in the 1500′s K, whereas the temperature gradient on the air side and the peak heat-release rate increase significantly from 0.01 m/s to 0.374 m/s due to the air blowing effect as U_a increases. For $U_a = 0.389$ m/s, the radial broadening and increase of $\dot{q}$, particularly on the air side, is apparent. In Fig. 3b, the axial velocity component of the local velocity at the reaction kernel (U_k) increases significantly as U_a increases from 0.01 m/s to 0.374 m/s. The radial component (V_k) changes its sign from negative to positive while the flame lifts off as U_a increases from 0.374 m/s to 0.389 m/s.

Fig. 4 shows the calculated axial variations of the temperature, heat-release rate, axial, and radial velocity components vertically across the reaction kernel. In Fig. 4a, since the temperature profile crosses vertically the reaction kernel of the outwardly inclined flame, the temperature reaches its maximum value slightly downstream on the fuel side of the flame. The maximum temperatures at $U_a = 0.01$ m/s, 0.374 m/s, and 0,389 m/s are 1567 K, 1755 K, and 1804 K, respectively. The temperature gradient increases as well while U_a increases from 0.01 m/s to 0.374 m/s. In Fig. 4b, the axial velocity at $U_a = 0.01$ m/s increases as approaching the reaction kernel due to the longitudinal thermal expansion by the temperature rise, whereas it shows deceleration at $U_a = 0.374$ m/s and 0.389 m/s due to lateral expansion. The minimum axial velocity flowing into the reaction kernel are 0.212 m/s and 0.235 m/s at $U_a = 0.374$ m/s and 0.389 m/s, respectively. The radial velocity changes its sign from the negative (inward) to positive (outward) direction as the flame base shifts outwardly.

Fig. 5 shows the radial and axial variations of the calculated species mole fractions (X_i) and temperature across the reaction kernel of the attached flame at $U_a = 0.01$ m/s (see Fig. 2a). In Fig. 5a, the radial distributions of species mole fractions exhibit the typical diffusion flame structure except that the oxygen concentration is high on the fuel side due to the upward airflow parallel to the burner wall. The outer surface of the burner tube is located at $r = 0.5$ mm, and thus the reaction kernel resides 0.57 mm away from the burner rim. The heavier-than-air n-butane (n-C_4H_{10}) spills out the fuel tube and diffuses back against the upward flow as well as in the radial direction. The fuel decomposes to smaller hydrocarbon fragments, including C_2H_4, C_3H_6, CH_4, C_2H_6, C_2H_2, CH_3, and C_4H_8, and partially oxidized species CH_2O, CH_2CO, CH_3CHO and so on. The oxygen diffuses from the air side as well as convection as described below. The oxygen mole fraction at the reaction kernel is 0.033. The chain carrier radicals (H, OH, and O) are formed slightly on the air side of the temperature peak and diffuse toward the reaction kernel, thus promoting the hydrocarbon decomposition and oxidation processes to form the intermediates H_2 and CO, and the products H_2O and CO_2 eventually.

In Fig. 5b, the axial distributions exhibit unique structure. Although there are some features of premixing that the mole fraction of oxygen decreases

Please cite this article as: F. Takahashi, L. Smith, D.T. Souza et al., Critical conditions at liftoff limit of a laminar N-butane-air jet diffusion flame, Proceedings of the Combustion Institute, https://doi.org/10.1016/j.proci.2022.07.037

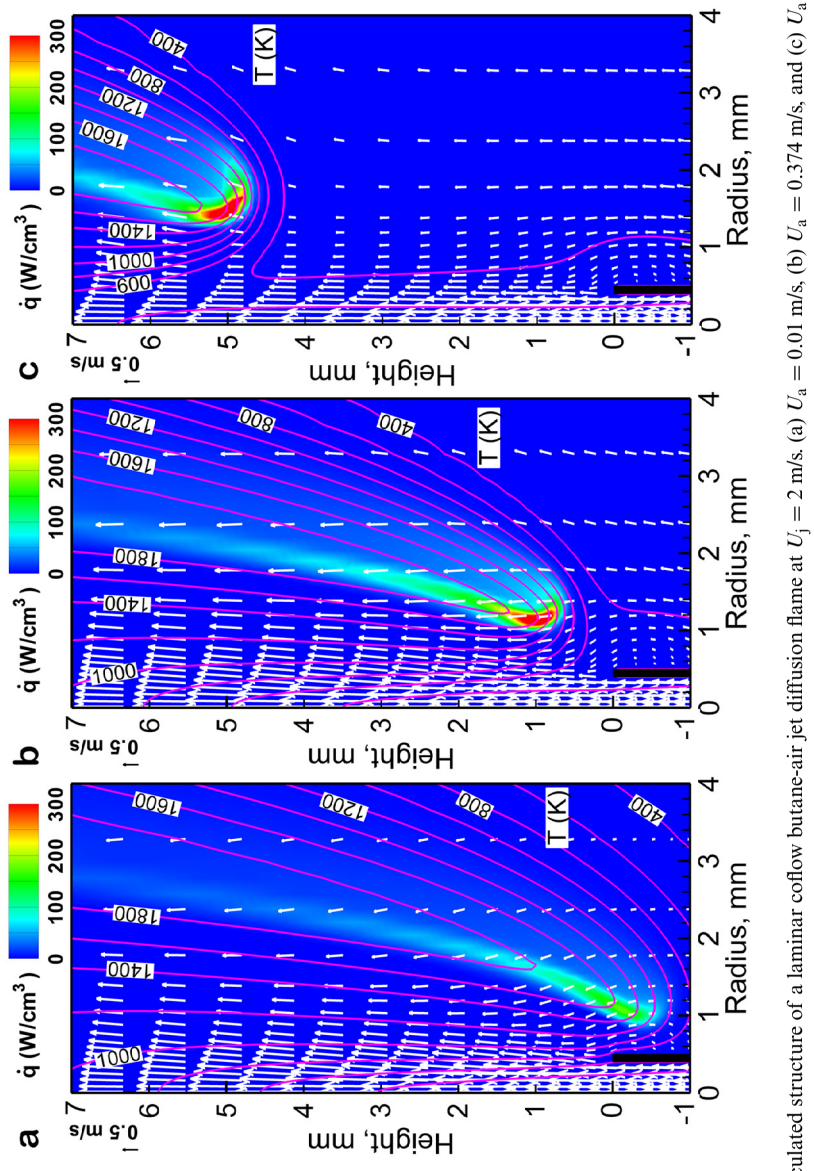

Fig. 2. Calculated structure of a laminar coflow butane-air jet diffusion flame at $U_j = 2$ m/s. (a) $U_a = 0.01$ m/s, (b) $U_a = 0.374$ m/s, and (c) $U_a = 0.389$ m/s.

Please cite this article as: F. Takahashi, L. Smith, D.T. Souza et al., Critical conditions at liftoff limit of a laminar N-butane-air jet diffusion flame, Proceedings of the Combustion Institute, https://doi.org/10.1016/j.proci.2022.07.037

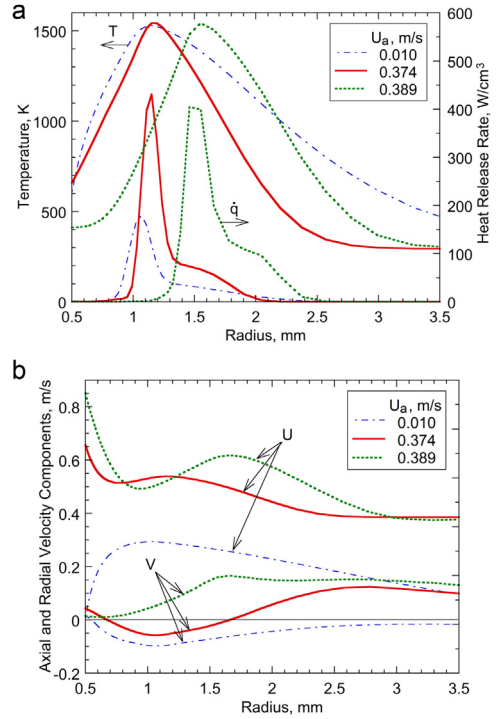

Fig. 3. Calculated radial variations of (a) temperature, heatrelease rate, and (b) axial and radial velocity components across the reaction kernel of a n-butane diffusion flame at $U_j = 2$ m/s.

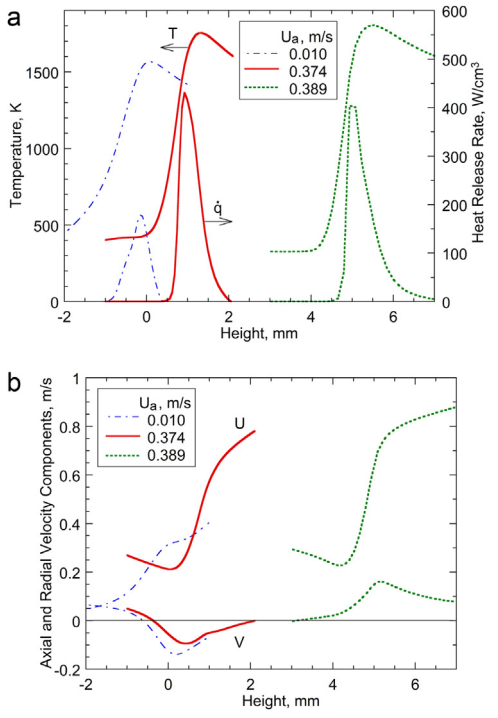

Fig. 4. Calculated axial variations of (a) temperature, heatrelease rate, and (b) axial and radial velocity components across the reaction kernel of a n-butane diffusion flame at $U_j = 2$ m/s.

downstream (left to right) and some fuel components (n-C_4H_{10} and C_2H_4) exist, their concentrations are too low to form a flammable mixture. On the other hand, a lot more hydrocarbon fuel and fragments (C_2H_4, C_2H_2, CH_4, CH_3, CH_2CO, CH_2O, C_2H_6, and n-C_4H_{10}) diffuse from the downstream and react with the radicals. Since the flame zone is inclined outwardly at the reaction kernel (see Fig. 2a), the downstream is on the fuel side of the flame, and thus diffusion-type combustion occurs in the axial as well as radial directions around the reaction kernel, except the lower side. Therefore, the attached flame at a very low coflow air velocity burns predominantly in the diffusion-type combustion possess.

Fig. 6 shows the structure across the reaction kernel of the near-limit flame at $U_a = 0.374$ m/s (see Fig. 2b). In Fig. 6a, the radial distributions of species mole fractions are like those in the attached flame (Fig. 5a), except that the concentrations of the n-C_4H_{10} is much higher since the flame base resides slightly above the jet exit. The oxygen mole fraction at the reaction kernel is 0.059. In Fig. 6b, the axial distributions are also like those in the attached flame (Fig. 5b) with the unique feature in the downstream. However, the upstream structure has much more premixed nature, except that the maximum n-C_4H_{10} mole fraction in the upstream is still low (< 0.0056), which is below the lean flammability limit (0.018) of the n-butane-air mixture.

Fig. 7 shows the structure across the reaction kernel of the flame in the lifting process at $U_a = 0.374$ m/s (see Fig. 2c). Both radial and axial profiles are similar to the near-limit case (Fig. 6), except that the n-C_4H_{10} mole fraction upstream reaches the maximum of 0.0187 at $z = 4.02$ mm, thus barely exceeding the lean flammability limit. The results apparently show the transition from the diffusion-combustion dominated attached flame base to premixed-combustion prevailing lifted flame.

4.3. Flame characteristics

Fig. 8 shows the effects of the coflow air velocity on the calculated coordinates (z_k and $y_k = r_k - 0.5$ mm) and velocity components at the reaction kernel. As U_a is increased from 0.01 to 0.374 m/s (the near-limit condition), z_k increases slightly from -0.15 mm to 0.92 mm, and thus the reaction kernel moves below to above the burner rim (see Fig. 2a and b). On the other hand, the distance from the burner surface y_k decreases slightly from 0.07 mm to 0 (at $U_a = 0.24$ m/s) inwardly and then in-

Please cite this article as: F. Takahashi, L. Smith, D.T. Souza et al., Critical conditions at liftoff limit of a laminar N-butane-air jet diffusion flame, Proceedings of the Combustion Institute, https://doi.org/10.1016/j.proci.2022.07.037

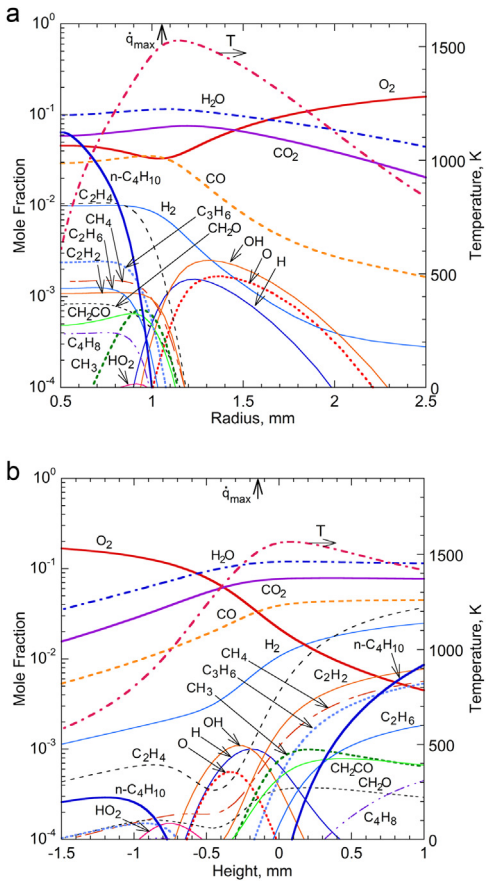

Fig. 5. Calculated (a) radial and (b) axial variations of species mole fraction and temperature across the reaction kernel of a n-butane diffusion flame at $U_j = 2$ m/s and $U_a = 0.01$ m/s. $z_k = -0.15$ mm, and $r_k = 1.07$ mm.

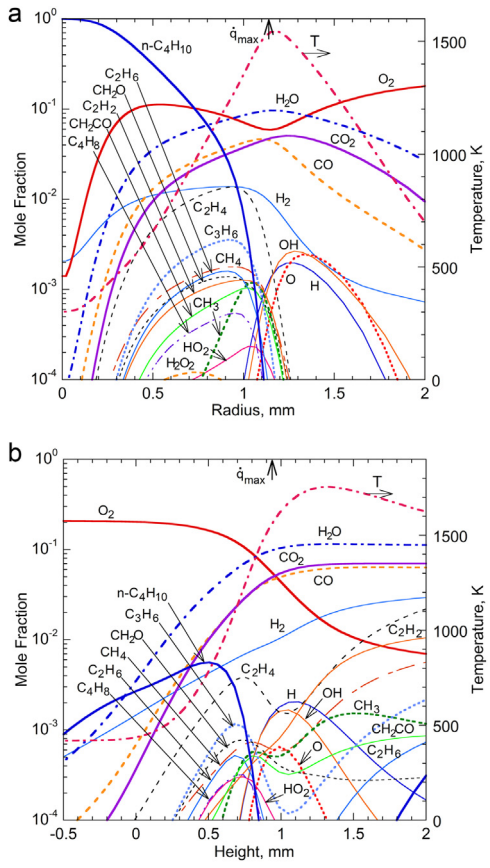

Fig. 6. Calculated (a) radial and (b) axial variations of species mole fraction and temperature across the reaction kernel of a n-butane diffusion flame at $U_j = 2$ m/s and $U_a = 0.374$ m/s. $z_k = 0.92$ mm and $r_k = 1.14$ mm.

creases to 0.15 mm outwardly. From $U_a = 0.374$ m/s to 0.389 m/s, both z_k and y_k increase rapidly to 4.94 mm and 0.46 mm, respectively (see Fig. 2b and c). The computational results for up to $U_a = 0.4$ m/s are reported here since the further increase pushes the reaction kernel into a region with a coarser grid spacing in the radial direction.

The incoming flow velocity around the flame base is important to diffusion flame stability as it represents the reciprocal of the residence time through the reaction kernel. Fig. 8 also includes the calculated axial (U_k), radial (V_k), and total ($|v_k|$) velocities at the reaction kernel. U_k increases linearly as U_a increases from 0.01 m/s to 0.374 m/s and increases more rapidly for higher U_a. The radial component (V_k) is nearly constant around −0.12 m/s over a wide range of U_a up to 0.374 m/s and then changes its sign from negative to positive while the flame lifts off at higher U_a. Variations in the behavior of z_k and r_k correlate with the velocity components. As the magnitude of V_k increases, the flame base is pushed against the burner rim and thus y_k decreases, while the base moves slightly up due to an increase in U_k. Since V_k is an order of magnitude smaller than U_k, the magnitude of the velocity vector $|v_k|$ is a little larger than U_k. Even in the near-quiescent environment, $|v_k|$ is 0.3 m/s due to the buoyancy-induced flow by the gravity of Earth. The previous computation for methane and ethane flames in microgravity revealed [16,18] that $|v_k|$ was 0.0056 and 0.0054 m/s, respectively, under the near-quiescent environment ($U_a = 0.001$ m/s).

Fig. 9 shows the calculated reaction kernel temperature (T_k), local equivalence ratio (ϕ_k), and heat-release rate ($\dot{q}_k$). For the pre-lift range of U_a from 0.01 m/s to 0.374 m/s, T_k maintains at ≈1555 K (standard deviation: 22.4 K), ϕ_k remains at ≈0.80 (standard deviation: 0.03), and $\dot{q}_k$ increases linearly from 178.8 W/cm^3 to 430.8 W/cm^3.

To determine the critical condition controlling the stability of diffusion flames, a local Damkhöler number (Da), i.e., a ratio of the residence time (τ_{res}) and the chemical reaction time (τ_{chem}), has

Please cite this article as: F. Takahashi, L. Smith, D.T. Souza et al., Critical conditions at liftoff limit of a laminar N-butane-air jet diffusion flame, Proceedings of the Combustion Institute, https://doi.org/10.1016/j.proci.2022.07.037

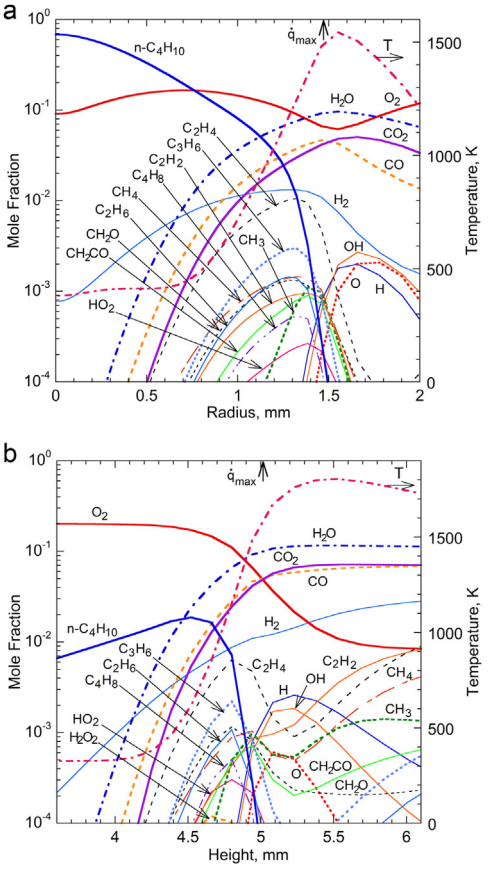

Fig. 7. Calculated (a) radial and (b) axial variations of species mole fraction and temperature across the reaction kernel of a n-butane diffusion flame at $U_j = 2$ m/s and $Ua = 0.389$ m/s. $z_k = 4.94$ mm, and $r_k = 1.46$ mm.

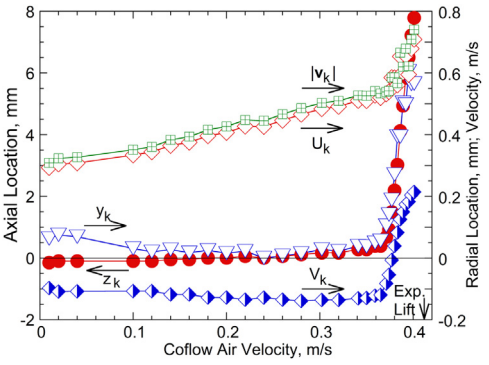

Fig. 8. Calculated reaction-kernel height from the burner exit (z_k), radius from the burner rim ($y_k = r_k - 0.5$), axial (U_k) and radial (V_k) velocity components and total velocity ($|v_k|$) at the reaction kernel of a n-butane flame at $U_j = 2$ m/s.

been considered [15,16,18] as a metric for the flame strength of the reaction kernel. As a quantity related to Da, $\dot{q}_k/|v_k|$ has been used previously [15,16,18] and, more recently [32], $(\dot{q}_k)^{1/2}/|v_k|$ has been introduced. As the flame base lifts off the burner rim, premixed combustion prevails the reaction kernel. The classic theory of premixed flame by Mallard and Le Chatelier derived [39] the total flame thickness (δ_L), which includes the preheat and reaction zones, and the laminar flame speed (S_L), respectively, as $\delta_L = (\lambda/[c_p\dot{\omega}])^{1/2}$ and $S_L = [(\lambda/\rho c_p)(\dot{\omega}/\rho)]^{1/2} = (\alpha\dot{\omega}/\rho)^{1/2}$ where λ is the thermal conductivity, c_p is the specific heat, ρ is the density, α is the thermal diffusivity, and $\dot{\omega}$ is the reaction rate (g/cm^{3}s). The residence time can be evaluated as the time for the fluid element to pass through the flame zone, i.e., $\tau_{res} = \delta_L/|v_k| = (\lambda/[c_p\dot{\omega}])^{1/2}/|v_k|$. The chemical reaction time can be determined as the time to consume the reactant in the flame zone, i.e., $\tau_{chem} = \rho/\dot{\omega}$. Therefore, the local Damkhöler number can be defined as $Da = \tau_{res}/\tau_{chem} = (\delta_L/|v_k|)/(\rho/\dot{\omega}) = [(\lambda/[c_p\dot{\omega}])^{1/2}/|v_k|] = (\alpha\dot{\omega}/\rho)^{1/2}/|v_k| = S_L/|v_k|$. By assuming that the overall heat release rate is proportional to the calculated heat-release rate at the reaction kernel, $\dot{Q} \sim \dot{q}_k$, where Q is the heat of reaction per unit mass, the local Damkhöler number is Da $\sim (\dot{q}_k)^{1/2}/|v_k|$. It is interesting that the derivation shows Da $= S_L/|v_k|$. The quantity $(\dot{q}_k)^{1/2}/|v_k|$ was introduced previously [32] since the laminar flame speed of premixed flames is proportional to the square-root of the reaction rate.

Fig. 10 shows the variations in $\dot{q}_k/|v_k|$ and $(\dot{q}_k)^{1/2}/|v_k|$ as a function of U_a. As U_a is increased from 0.001 m/s to 0.374 m/s, the quantity $\dot{q}_k/|v_k|$ gradually increases from 5.8 to 7.9 (J/cm^4), while $(\dot{q}_k)^{1/2}/|v_k|$ decreases gradually from 0.43 to a nearly constant level of $\approx$0.38 (Js/cm^5)$^{1/2}$. As U_a increases further, both $\dot{q}_k/|v_k|$ and $(\dot{q}_k)^{1/2}/|v_k|$ drops abruptly, as the flame detaches and lifts off from the burner rim. Therefore, $(\dot{q}_k)^{1/2}/|v_k| = 0.38$ (Js/cm^5)$^{1/2}$ can be regarded as a critical threshold value for the flame liftoff limit. A further increase in U_a drives the flame base downstream rapidly (see Fig. 8).

This result suggests that the reaction kernel shifted downstream to seek a location where a subtle balance between the residence time and the reaction time can be achieved. As the flame base lifted higher in the higher velocity field, it becomes difficult to obtain the balance as Da falls, thus leading eventually to blowoff unless a turbulent lifted flame base is formed.

The behavior of $\dot{q}_k/|v_k|$ and $(\dot{q}_k)^{1/2}/|v_k|$ are consistent with the extinguishment of cup-burner coflow diffusion flames of methane and propane with fire-extinguishing agents (C_2HF_5, $C_2HF_3Cl_2$, $C_3H_2F_3Br$, and $C_6F_{12}O$) [27,30,32] and the chemically passive agents [23,26]. In fact, the critical $(\dot{q}_k)^{1/2}/|v_k|$ value at extinguishment for $C_6F_{12}O$

Please cite this article as: F. Takahashi, L. Smith, D.T. Souza et al., Critical conditions at liftoff limit of a laminar N-butane-air jet diffusion flame, Proceedings of the Combustion Institute, https://doi.org/10.1016/j.proci.2022.07.037

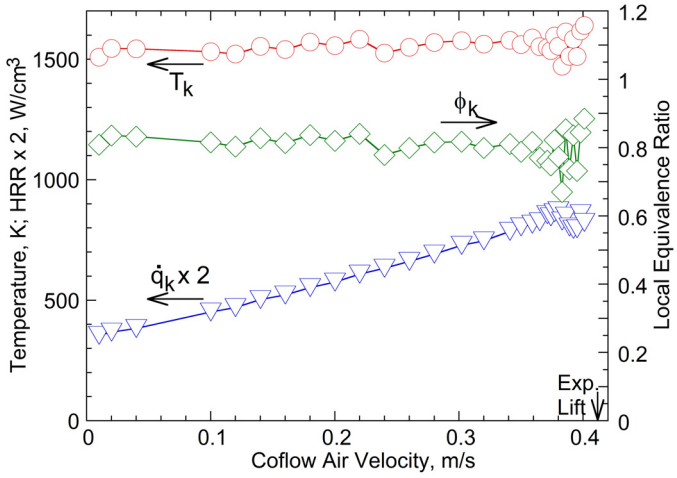

Fig. 9. Calculated temperature (Tk), local equivalence ratio (φ k), and heat-release rate ($\dot{q}_k$) at the reaction kernel of a nbutane diffusion flame at Uj = 2 m/s.

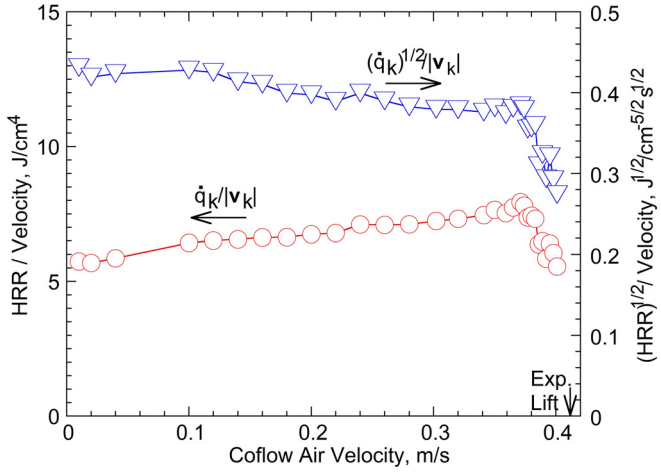

Fig. 10. Calculated variations of $(\dot{q}_k/|\mathbf{v}_k|)$ and $(\dot{q}_k)^{1/2}/|\mathbf{v}_k|$ in relation to the local Damkhöler number at the reaction kernel of a n-butane diffusion flame at Uj = 2 m/s.

is ≈0.4 $(\mathrm{Js/cm^5})^{1/2}$, and it is consistent with the present work.

It is important to notice that although the critical Damkhöler number is introduced as the flame blowoff criterion, the flame base is still vigorously burning at the limit, in contrast to chemical extinction phenomena.

5. Conclusions

The effects of the coflow air velocity on the structure, stabilization, and detachment of laminar jet diffusion flames have been investigated using n-butane, for the first time, as the fuel. The stability limits (liftoff and blowout) are measured and reported as a fuel jet velocity vs. coflow air velocity plot. The full-chemistry computation revealed the detailed physical and chemical flame structure. A peak-reactivity spot reaction kernel, possessing the hybrid diffusion-premixed fuel-lean (ϕ ≈0.8) combustion characteristics at ≈1560 K, at the flame base plays a critical role in the stability of coflow diffusion flames. The increased airflow pushes the flame base inwardly onto the burner rim and upwardly slightly above the jet exit, causing the air (oxygen) blowing effect, enhances the premixed nature, and thus increases the heat-release rate of the flame-holding reaction kernel. For the n-butane flame base, the local equivalence ratio is larger than methane or propane probably because of its proximity to the burner rim. The flame

Please cite this article as: F. Takahashi, L. Smith, D.T. Souza et al., Critical conditions at liftoff limit of a laminar N-butane-air jet diffusion flame, Proceedings of the Combustion Institute, https://doi.org/10.1016/j.proci.2022.07.037

base detaches from the burner rim as the newly defined local Damkhöler number at the reaction kernel, i.e., a ratio of the residence time and the reaction time, represented by $(\dot{q}_k)^{1/2}/|v_k|$, decreases to a critical threshold value of ≈ 0.38 $(Js/cm^5)^{1/2}$. This value coincides with the blowoff-limit conditions of methane and propane cup-burner flames by fire-extinguishing agents. The calculated coflow air velocity at liftoff is ≈0.38 m/s at the fuel velocity of 2 m/s, which is consistent with an extrapolated measured value of 0.41 m/s. Because any hydrocarbon fuel decomposes eventually to the same fragments (C_1 and C_2, mainly acetylene, ethylene, and methane), which are oxidized locally in the reaction zone, the structure of the reaction kernel is similar. The *local* Damköhler number, determined quantitatively for the first time, are significant as they are decisive whether the flame base of a laminar jet diffusion flame moves farther away downstream (the liftoff-limit condition), independent of the type of fuel and burner geometry used thus far.

Declaration of Competing Interest

We wish to confirm that there are no known conflicts of interest associated with this publication and there has been no significant financial support for this work that could have influenced its outcome.

Acknowledgements

This work at Case Western Reserve University was supported by the NASA Space Life and Physical Sciences Research and Applications Division (SLPSRA) under the cooperative agreement (Award No. 80NSSC18M0040, Technical Officer: Dennis Stocker) and the National Science Foundation (Award No. 1842067, Program Officers: Harsha Chelliah and John Daily).

References

[1] K. Wohl, N.M. Kapp, C. Gazley, The stability of open flames, Proc. Combust. Inst. 3 (1949) 3–21.
[2] B. Lewis, G. von Elbe, in: Combustion, Flames, and Explosions of Gases, second ed., Academic Press, New York, 1961, p. 237.
[3] A.G. Gaydon, H.G. Wolfhard, in: Flames—Their Structure, Radiation and Temperature, fourth ed., Chapman and Hall, London, 1979, p. 39.
[4] K. Robson, M.J.G. Wilson, The stability of laminar diffusion flames of methane, Combust. Flame 13 (1969) 626–634.
[5] T. Takeno, Y. Kotani, An experimental study on the stability of jet diffusion flames, Acta Astronaut. 2 (1975) 999–1008.
[6] T. Kawamura, K. Asato, T. Mazaki, Structure analysis of the stabilizing region of plane, laminar fuel-jet flames, Combust. Sci. Technol. 22 (1980) 211.
[7] F. Takahashi, M. Mizomoto, S. Ikai, N. Futaki, Lifting mechanism of free jet diffusion flames, Proc. Combust. Inst. 20 (1985) 295–302.
[8] F. Takahashi, M. Mizomoto, S. Ikai, Structure of the stabilizing region of a laminar jet diffusion flame, J. Heat Trans. 110 (1988) 182.
[9] S.H. Chung, B.J. Lee, On the characterization of laminar lifted flames in a nonpremixed jet, Combust. Flame 86 (1991) 62–72.
[10] F. Takahashi, W.J. Schmoll, Lifting criteria of jet diffusion flames, Proc. Combust. Inst. 23 (1991) 677–683.
[11] B.J. Lee, S.H. Chung, Stabilization of lifted tribrachial flames in a laminar nonpremixed jet, Combust. Flame 109 (1997) 163–172.
[12] S.H. Chung, Stabilization, propagation and instability of tribrachial triple flames, Proc. Combust. Flame 31 (2007) 877–892.
[13] F. Takahashi, W.J. Schmoll, V.R. Katta, Attachment mechanisms of diffusion flames, Proc. Combust. Inst. 27 (1998) 675–684.
[14] F. Takahashi, V.R. Katta, Chemical kinetic structure of the reaction kernel of methane jet diffusion flames, Combust. Sci. Technol. 155 (2000) 243–279.
[15] F. Takahashi, V.R. Katta, A reaction kernel hypothesis for the stability limit of methane jet diffusion flames, Proc. Combust. Inst. 28 (2000) 2071–2078.
[16] F. Takahashi, V.R. Katta, Reaction kernel structure and stabilizing mechanisms of jet diffusion flames in microgravity, Proc. Combust. Inst. 29 (2002) 2509–2518.
[17] F. Takahashi, V.R. Katta, Structure of propagating edge diffusion flames in hydrocarbon fuel jets, Proc. Combust. Inst. 30 (2005) 375–382.
[18] F. Takahashi, V.R. Katta, Further studies of the reaction kernel structure and stabilization of jet diffusion flames, Proc. Combust. Inst. 30 (2005) 383–390.
[19] A.M. Briones, S.K. Aggarwal, V.R. Katta, A numerical investigation of flame liftoff, stabilization, and blowout, Phys. Fluids 18 (2006) 043603.
[20] T.S. Cheng, C.-P. Chen, C.-S. Chen, Y.-H. Li, C.-Y. Wu, Y.-C. Chao, Characteristics of microjet methane diffusion flames, Combust. Theory Model. 10 (5) (2006) 861–881.
[21] F. Takahashi, G.T. Linteris, V.R. Katta, Vortex-coupled oscillations of edge diffusion flames in coflowing air with dilution, Proc. Combust. Inst. 31 (2007) 1575–1582.
[22] F. Takahashi, G.T. Linteris, V.R. Katta, Extinguishment mechanisms of coflow diffusion flames in a cup-burner apparatus, Proc. Combust. Inst. 31 (2007) 2721–2729.
[23] F. Takahashi, G.T. Linteris, V.R. Katta, Extinguishment of methane diffusion flames by carbon dioxide in coflow air and oxygen-enriched microgravity environments, Combust. Flame 155 (1–2) (2008) 37–53.
[24] J. Min, F. Baillot, A. Wyzgolik, E. Domingues, M. Talbaut, B. Patte-Rouland, C. Galizzi, Impact of $CO_2/N_2/Ar$ addition on the internal structure and stability of nonpremixed CH_4/air flames at lifting, Combust. Sci. Technol. 182 (11–12) (2010) 1782–1804.
[25] Z. Li, R.-H. Chen, T.X. Phuoc, Effects of multicomponent diffusion and heat release on laminar diffusion flame liftoff, Combust. Flame 157 (2010) 1484–1495.

Please cite this article as: F. Takahashi, L. Smith, D.T. Souza et al., Critical conditions at liftoff limit of a laminar N-butane-air jet diffusion flame, Proceedings of the Combustion Institute, https://doi.org/10.1016/j.proci.2022.07.037

[26] F. Takahashi, G.T. Linteris, V.R. Katta, Extinguishment of methane diffusion flames by inert gases in coflow air and oxygen-enriched microgravity environments, Proc. Combust. Inst. 33 (2011) 2531–2538.
[27] F. Takahashi, V.R. Katta, G.T. Linteris, Combustion inhibition and enhancement of cup-burner flames by CF_3Br, C_2HF_5, $C_2HF_3Cl_2$, and $C_3H_2F_3Br$, Proc. Combust. Inst. 35 (2015) 2741–2748.
[28] S. Deng, P. Zhao, M.E. Mueller, C.K. Law, Autoignition-affected stabilization of laminar nonpremixed DME/air coflow flames, Combust. Flame 162 (2015) 3437–3445.
[29] D. Giassi, S. Cao, B.A.V. Bennett, D.P. Stocker, F. Takahashi, M.D. Smooke, M.B. Long, Analysis of CH^* concentration and flame heat release rate in laminar coflow diffusion flames under microgravity and normal gravity, Combust. Flame 167 (2016) 198–206.
[30] F. Takahashi, V.R. Katta, G.T. Linteris, V.I. Babushok, A computational study of extinguishment and enhancement of propane cup-burner flames by halon and alternative agents, Fire Safety J 91 (2017) 688–694.
[31] J. Gao, A. Hossain, Y. Nakamura, Flame base structures of micro-jet hydrogen/methane diffusion flames, Proc. Combust. Inst. 36 (2017) 4209–4216.
[32] F. Takahashi, V.R. Katta, V.I. Babushok, G.T. Linteris, Numerical and experimental studies of extinguishment of cup-burner flames by $C_6F_{12}O$, Proc. Combust. Inst. 38 (2021) 4645–4653.
[33] V.R. Katta, L.P. Goss, W.M. Roquemore, Numerical investigations of transitional H_2/N_2 jet diffusion flames, AIAA J. 32 (1) (1994) 84.
[34] W.M. Roquemore, V.R. Katta, Role of flow visualization in the development of UNICORN, J. Visualization 2 (3) (2000) 257–272 4.
[35] J.O. Hirschfelder, C.F. Curtis, R.B. Bird, The Molecular Theory of Gases and Liquids, Wiley, New York, 1954.
[36] R.S. Barlow, A.N. Karpetis, J.H. Frank, J.-.Y. Chen, Scalar profiles and NO formation in laminar opposed-flow partially premixed methane/air flames, Combust. Flame 127 (3) (2001) 2102–2118.
[37] Chemical-Kinetic Mechanisms for Combustion Applications, San Diego Mechanism web page, Mechanical and Aerospace Engineering (Combustion Research), University of California at San Diego (http://combustion.ucsd.edu).
[38] J.C. Prince, C. Trevino, F.A. Williams, A reduced reaction mechanism for the combustion of n-butane, Combust. Flame 175 (1) (2017) 27–33.
[39] I. Glassman, R.A. Yetter, N.G. Glumac, Combustion (2015) 157.

Please cite this article as: F. Takahashi, L. Smith, D.T. Souza et al., Critical conditions at liftoff limit of a laminar N-butane-air jet diffusion flame, Proceedings of the Combustion Institute, https://doi.org/10.1016/j.proci.2022.07.037